SCIENTIFIC OASIS

Spectrum of Mechanical Engineering and Operational Research

Journal homepage: www.smeor-journal.org
eISSN: 3042-0288

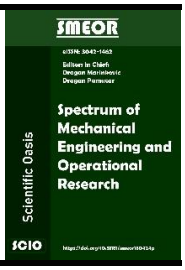

The Effect of a Fully Asymmetric Discontinuity in the Elastic Layer of a Geometrically Nonlinear Double-Beam Coupled Mechanical System

Dunja Milić[1,*], Jian Deng[2], Deli Li[3], Vladimir Stojanović[1,2]

[1] Department of Theoretical and Applied Mechanics, Faculty of Mechanical Engineering, University of Niš, Serbia
[2] Department of Civil Engineering, Lakehead University, Ontario, Canada
[3] Department of Mathematical Sciences, Lakehead University, Ontario, Canada

ARTICLE INFO

Article history:
Received 14 July 2024
Received in revised form 20 November 2024
Accepted 17 December 2024
Available online 22 December 2024

Keywords:
p-version of FEM; Nonlinear vibrations; Coupled beam system; Asymmetric layer; Newmark method.

ABSTRACT

This paper presents the effect of an antisymmetric discontinuity in a Winkler nonlinear elastic layer and compares it with the case of a double Timoshenko beam system without discontinuities. The effects of geometric nonlinearity are considered, and the obtained results represent a time-domain analysis. A modified p-version finite element method is applied to analyse the vibrations of mechanical systems with discontinuities. The main contribution of this work is a comparative analysis of a double beam system without discontinuities and a double beam system with an antisymmetric discontinuity in the Winkler elastic layer. The study demonstrates significant deviations in the beam response under a concentrated periodic external force when an antisymmetric discontinuity is present. Its qualitative and quantitative characteristics are illustrated through time histories, showing amplitude variations in the steady-state oscillation regime. Forced vibrations in the time domain are analysed using the Newmark direct integration method. The cases of deviations in the antisymmetric model are explained, highlighting their potential applications in technical practice as well as in the field of deformable bodies and structures.

1. Introduction

The study of vibrations and dynamic behavior in coupled beams or plates has been extensively explored due to its practical significance in mechanical and civil engineering, particularly as continuous vibration absorbers (Rezaei *et al.* [1], Ari and Faal [2]). Coupled mechanical models also play a crucial role in aerospace engineering, sandwich structures, and laminated composite systems widely used in engineering practice (Zhang *et al.* [3], Kennedy *et al.* [4], Stojanović *et al.* [5]). Among these, elastically connected structures are frequently represented by coupled beam models, especially for vibration analysis where the elastic layer functions as a type of foundation or support (Hao *et al.* [6], Zhang *et al.* [7], Li and Gong [8], Ghomshei [9]). For instance, Bochicchio *et al.* [10] investigated damped transverse vibrations of a double-beam system elastically coupled and

* *Corresponding author.*
E-mail address: dunja1994milic@gmail.com

https://doi.org/10.31181/smeor21202529

subjected to compressive axial loading, with each beam assumed to be elastic, extensible, and supported at its ends. Hajarolasvadi and Elbanna [11] examined parallel beams connected at discrete points, ensuring deformation and force compatibility, and conducted a parametric study on how material properties and connection compliance affect the system's dynamic band structure. Adam and Furtmüller [12] analyzed composite beams with bonded layers experiencing interlayer slip during moderate vibrations, employing nonlinear strain-displacement relations to improve model accuracy. Understanding the dynamic behavior of coupled structures contributes significantly to identifying physical phenomena arising from elastic connections, which may vary in their realization (Palmeri and Adhikari [13], Xin *et al.* [14], Zhou *et al.* [15]). These variations include different models of elastic layers, ranging from continuous distributions to cases with localized damage or geometric irregularities like discontinuities and curvatures. Although works addressing the dynamic or stochastic stability of elastically connected beams exist, they are considerably fewer (Mazur-Śniady *et al.* [16], Mohammadzadeh *et al.* [17]). Analytical studies, while valuable for understanding fundamental dynamic principles, often neglect practical scenarios such as beams with damaged elastic layers, discontinuities, or geometric deviations. Recent research underscores the importance of discontinuities in coupled structures. For example, Di Lorenzo *et al.* [18] examined the dynamic flexural behavior of layered beams with elastic bonding, incorporating abrupt changes in response variables at support and joint points, while Juarez and Ayala [19] developed a variational formulation to model beams with localized strain zones representing dislocations and hinges. In another example, Srikarun *et al.* [20] analyzed sandwich beams with functionally graded porous cores under distributed loads using advanced deformation theories, while Songsuwan *et al.* [21] explored the nonlinear transient response of similar beams under moving loads, employing Newmark's time-integration method for convergence. Shear effects are also critical in analyzing such systems, as shown by Bitar *et al.* [22], who proposed a Timoshenko beam model with embedded rotation discontinuities to simulate plastic hinges and crack openings. The p-version finite element method (FEM) is a powerful tool for modeling vibrational behavior in spatially complex systems (Szabó and Babuška [23], Petyt [24], Han and Petyt [25], Bardell [26]). When accounting for geometrically nonlinear effects in shear-deformable beams and elastic layers with discontinuities, an improved p-version FEM is particularly effective. As demonstrated in Stojanović *et al.* [27], this method captures the altered vibration dynamics introduced by discontinuities. Timoshenko beam theory, known for incorporating shear deformation and rotary inertia, remains a key framework for studying coupled systems and beams on elastic foundations. De Rosa [28] analyzed the vibrations of a shear-deformable beam on a Pasternak foundation, deriving frequency equations for various boundary conditions. Similarly, Ariaei *et al.* [29] investigated the dynamic response of multiple elastically connected beams, using modal analysis to decouple and solve the governing equations.

This paper focuses on a specific class of coupled beam models, examining the effect of a fully antisymmetric discontinuity in the elastic layer connecting two beams. The analysis includes transverse shear effects, geometric nonlinearity, and provides a comparison with a nonlinear double-beam system model that does not contain a discontinuity in the Winkler elastic layer. The primary objective is to investigate the impact of a fully antisymmetric discontinuity in the elastic layer on natural frequencies and nonlinear time-domain responses. The study analyzes steady-state regimes under harmonic excitation by a concentrated periodic force acting at the midpoint of the upper beam. The equations of motion are derived using the principle of virtual work and solved using the Newmark method. Model validation is performed by comparing the results with those obtained from ANSYS software [30].

2. Mathematical model

The Timoshenko beam system considered in this study features a rectangular cross-section. The analysis incorporates the effects of rotary inertia and shear deformation to model a coupled beam-beam or beam-arch configuration (Figure 1), which is elastically joined by a nonlinear layer exhibiting a discontinuity. To account for geometric nonlinearity arising from large deflections, the Timoshenko beam theory is utilized alongside the von Kármán plate theory adapted for beams. Additionally, the study examines a viscoelastically connected beam system with an asymmetric discontinuity and compares it to a classical double-beam configuration.

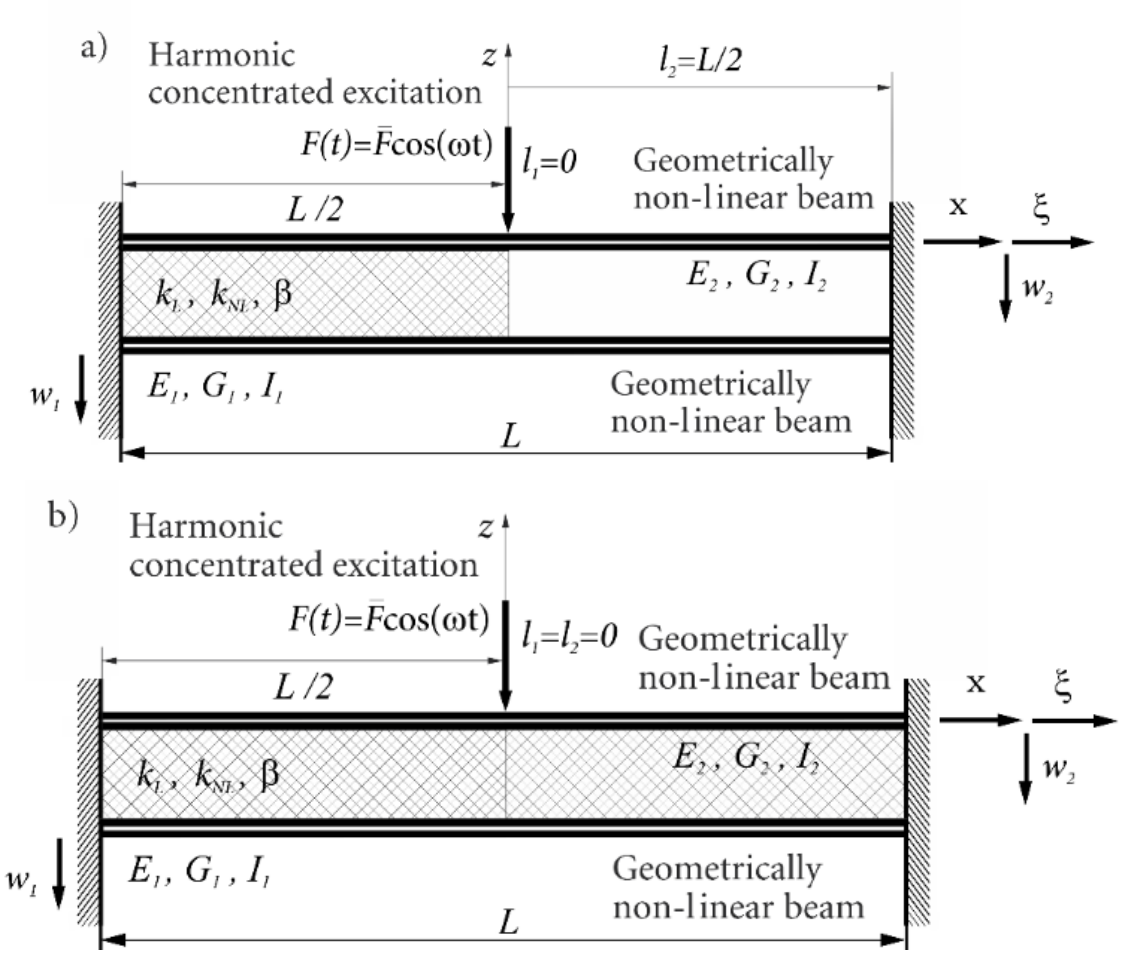

Fig. 1. Timoshenko geometrically non-linear beam system:
a) with asymmetric discontinuity; b) double-beam system

The dimensions of the beams are characterized by their length L, width b, and thickness h. The discontinuity within the Winkler layer is specified through the parameters l_1 and l_2 (as illustrated in Figure 1). The viscoelastic layer is described by its linear stiffness modulus k_L, nonlinear stiffness modulus k_{NL}, and damping coefficient β. Both the beams and the arch are assumed to be elastic and isotropic materials. The in-plane displacements u_1, u_2, along with the transverse displacements w_1 and w_2 at specific points of the arch and beam, are defined as follows

$$u_i(x,z,t) = u_i^0(x,t) + z\theta_i^0(x,t), \quad w_i(x,z,t) = w_i^0(x,t), \;\; i = 1,2 \tag{1}$$

In this context, w represents the displacement along the z -axis. A concentrated harmonic force is applied at the midpoint of the upper beam. The longitudinal strain at $z = 0$, ε_{x1}^{0}, can be expressed as follows

$$\varepsilon_{x1}^{0} = \frac{\partial u_1^0(x,t)}{\partial x} \tag{2}$$

A von Kármán framework is utilized in this study, incorporating the primary geometric nonlinearities. Accordingly, the longitudinal and shear strain expressions for both the curved arch and the straight beam are formulated as follows

$$\varepsilon_{x1} = \varepsilon_{x1}^{0} + \frac{1}{2}\left(\frac{\partial w_1^0}{\partial x}\right)^2 + z\frac{\partial \theta_1^0}{\partial x},\ \varepsilon_{x2} = \frac{\partial u_2^0(x,t)}{\partial x} + \frac{1}{2}\left(\frac{\partial w_2^0}{\partial x}\right)^2 + z\frac{\partial \theta_2^0}{\partial x}, \tag{3}$$

$$\gamma_{xz1} = \frac{\partial w_1^0}{\partial x} + \theta_1^0,\ \ \gamma_{xz2} = \frac{\partial w_2^0}{\partial x} + \theta_2^0 \tag{4}$$

The governing equations for materials exhibiting linear elasticity and isotropic properties can be expressed as follows

$$\sigma = \mathrm{D}\varepsilon \Leftrightarrow \begin{Bmatrix} \sigma_{x1} \\ \tau_{xz1} \\ \sigma_{x2} \\ \tau_{xz2} \end{Bmatrix} = \begin{bmatrix} E_1 & 0 & 0 & 0 \\ 0 & \lambda_1 G_1 & 0 & 0 \\ 0 & 0 & E_2 & 0 \\ 0 & 0 & 0 & \lambda_2 G_2 \end{bmatrix} \begin{Bmatrix} \epsilon_{x1} \\ \gamma_{xz1} \\ \varepsilon_{x2} \\ \gamma_{xz2} \end{Bmatrix} \tag{5}$$

In this context, E_1 and E_2 denote the Young's moduli corresponding to the lower and upper beams, respectively, while G_1 and G_2 represent their respective shear moduli. The parameters $\boldsymbol{\lambda_1}$ and $\boldsymbol{\lambda_2}$ are the shear correction factors, $\mathbf{D}$ is the matrix of elastic constants, and $\boldsymbol{\sigma}$ and $\boldsymbol{\varepsilon}$ are vectors containing the non-zero components of stress and strain, respectively. The shear moduli are defined as $E_i/(2(1+\nu_i))$, where ν_i is the Poisson's ratio for the material. In the p-version finite element method, the displacements of the mid-surface for each element are represented using the following formulation

$$\begin{Bmatrix} u_1^0(\xi,t) \\ w_1^0(\xi,t) \\ \theta_1^0(\xi,t) \\ u_2^0(\xi,t) \\ w_2^0(\xi,t) \\ \theta_2^0(\xi,t) \end{Bmatrix} = \mathrm{diag}\left\{[N^{u_1}]^{\mathrm{T}}, [N^{w_1}]^{\mathrm{T}}, \left[N^{\theta_1}\right]^{\mathrm{T}}, [N^{u_2}]^{\mathrm{T}}, [N^{w_2}]^{\mathrm{T}}, \left[N^{\theta_2}\right]^{\mathrm{T}}\right\} \begin{Bmatrix} \mathrm{q}_{u1}(t) \\ \mathrm{q}_{w1}(t) \\ \mathrm{q}_{\theta 1}(t) \\ \mathrm{q}_{u2}(t) \\ \mathrm{q}_{w2}(t) \\ \mathrm{q}_{\theta 2}(t) \end{Bmatrix} \tag{6}$$

By utilizing the principle of virtual work, expressed as $\begin{Bmatrix} \delta W_{\mathbf{in}(1)} + \delta W_{\mathbf{V}(1)} + \delta W_{\mathbf{ex}(1)} \\ \delta W_{\mathbf{in}(2)} + \delta W_{\mathbf{V}(2)} + \delta W_{\mathbf{ex}(2)} \end{Bmatrix} = \begin{Bmatrix} 0 \\ 0 \end{Bmatrix}$, the equations of motion for a geometrically nonlinear coupled system are formulated and can be expressed in the following manner

$$\begin{bmatrix} \mathrm{M}_{11} & 0 & 0 & 0 & 0 & 0 \\ 0 & \mathrm{M}_{12} & 0 & 0 & 0 & 0 \\ 0 & 0 & \mathrm{M}_{13} & 0 & 0 & 0 \\ 0 & 0 & 0 & \mathrm{M}_{21} & 0 & 0 \\ 0 & 0 & 0 & 0 & \mathrm{M}_{22} & 0 \\ 0 & 0 & 0 & 0 & 0 & \mathrm{M}_{23} \end{bmatrix} \begin{Bmatrix} \ddot{\mathrm{q}}_{u1} \\ \ddot{\mathrm{q}}_{w1} \\ \ddot{\mathrm{q}}_{\theta 1} \\ \ddot{\mathrm{q}}_{\mathrm{u}2} \\ \ddot{\mathrm{q}}_{w2} \\ \ddot{\mathrm{q}}_{\theta 2} \end{Bmatrix} +$$

$$+\tilde{\alpha} \left(\begin{bmatrix} \mathrm{K}_{11} & 0 & 0 & 0 & 0 & 0 \\ 0 & \mathrm{K}_{22(s)} + \mathrm{K}_{22(\gamma 11)} + \mathrm{K}_{22(k_L)}^{disc.} & \mathrm{K}_{23(\gamma 12)} & 0 & -\mathrm{K}_{22(k_L)}^{disc.} & 0 \\ 0 & \mathrm{K}_{32(\gamma 21)} & \mathrm{K}_{33(\gamma 22)} + \mathrm{K}_{33(0)} & 0 & 0 & 0 \\ 0 & 0 & 0 & \mathrm{K}_{44} & 0 & 0 \\ 0 & -\mathrm{K}_{22(k_L)}^{disc.} & 0 & 0 & \mathrm{K}_{55(\gamma 11)} + \mathrm{K}_{22(k_L)}^{disc.} & \mathrm{K}_{56(\gamma 12)} \\ 0 & 0 & 0 & 0 & \mathrm{K}_{65(\gamma 21)} & \mathrm{K}_{66(\gamma 22)} + \mathrm{K}_{66(0)} \end{bmatrix} \right) \begin{Bmatrix} \dot{\mathrm{q}}_{u1} \\ \dot{\mathrm{q}}_{w1} \\ \dot{\mathrm{q}}_{\theta 1} \\ \dot{\mathrm{q}}_{\mathrm{u}2} \\ \dot{\mathrm{q}}_{w2} \\ \dot{\mathrm{q}}_{\theta 2} \end{Bmatrix}$$

$$+\tilde{\beta} \left(\begin{bmatrix} \mathrm{M}_{11} & 0 & 0 & 0 & 0 & 0 \\ 0 & \mathrm{M}_{12} & 0 & 0 & 0 & 0 \\ 0 & 0 & \mathrm{M}_{13} & 0 & 0 & 0 \\ 0 & 0 & 0 & \mathrm{M}_{21} & 0 & 0 \\ 0 & 0 & 0 & 0 & \mathrm{M}_{22} & 0 \\ 0 & 0 & 0 & 0 & 0 & \mathrm{M}_{23} \end{bmatrix} \right) \begin{Bmatrix} \dot{\mathrm{q}}_{u1} \\ \dot{\mathrm{q}}_{w1} \\ \dot{\mathrm{q}}_{\theta 1} \\ \dot{\mathrm{q}}_{\mathrm{u}2} \\ \dot{\mathrm{q}}_{w2} \\ \dot{\mathrm{q}}_{\theta 2} \end{Bmatrix}$$

$$+ \begin{bmatrix} \mathrm{K}_{11} & 0 & 0 & 0 & 0 & 0 \\ 0 & \mathrm{K}_{22(s)} + \mathrm{K}_{22(\gamma 11)} + \mathrm{K}_{22(k_L)}^{disc.} & \mathrm{K}_{23(\gamma 12)} & 0 & -\mathrm{K}_{22(k_L)}^{disc.} & 0 \\ 0 & \mathrm{K}_{32(\gamma 21)} & \mathrm{K}_{33(\gamma 22)} + \mathrm{K}_{33(0)} & 0 & 0 & 0 \\ 0 & 0 & 0 & \mathrm{K}_{44} & 0 & 0 \\ 0 & -\mathrm{K}_{22(k_L)}^{disc.} & 0 & 0 & \mathrm{K}_{55(\gamma 11)} + \mathrm{K}_{22(k_L)}^{disc.} & \mathrm{K}_{56(\gamma 12)} \\ 0 & 0 & 0 & 0 & \mathrm{K}_{65(\gamma 21)} & \mathrm{K}_{66(\gamma 22)} + \mathrm{K}_{66(0)} \end{bmatrix} \begin{Bmatrix} \mathrm{q}_{u1} \\ \mathrm{q}_{w1} \\ \mathrm{q}_{\theta 1} \\ \mathrm{q}_{\mathrm{u}2} \\ \mathrm{q}_{w2} \\ \mathrm{q}_{\theta 2} \end{Bmatrix}$$

$$+ \begin{bmatrix} 0 & \mathrm{K}_{12(NL)} & 0 & 0 & 0 & 0 \\ \mathrm{K}_{21(NL)} & \mathrm{K}_{22(NL)} + \mathrm{K}_{22(k_{NL})}^{disc.} & 0 & 0 & -\mathrm{K}_{24(k_{NL})}^{disc.} & 0 \\ 0 & 0 & 0 & 0 & 0 & 0 \\ 0 & 0 & 0 & 0 & \mathrm{K}_{45(NL)} & 0 \\ 0 & -\mathrm{K}_{22(k_{NL})}^{disc.} & 0 & \mathrm{K}_{54(NL)} & \mathrm{K}_{55(NL)} + \mathrm{K}_{24(k_{NL})}^{disc.} & 0 \\ 0 & 0 & 0 & 0 & 0 & 0 \end{bmatrix} \begin{Bmatrix} \mathrm{q}_{u1} \\ \mathrm{q}_{w1} \\ \mathrm{q}_{\theta 1} \\ \mathrm{q}_{\mathrm{u}2} \\ \mathrm{q}_{w2} \\ \mathrm{q}_{\theta 2} \end{Bmatrix} = \begin{Bmatrix} 0 \\ 0 \\ 0 \\ 0 \\ F_{w2} \\ 0 \end{Bmatrix} \tag{7}$$

In the system, the vector $\{0,\ 0,\ 0,\ 0,\ \mathbf{F}_{w2}, 0\}$ represents the generalized external forces. The matrices $\mathbf{M}_{**}$, $\mathbf{K}_{**}$, and $\mathbf{K}_{**(r,\gamma,k_L)}$ are constant and contribute to the linear terms within the equations of motion. Quadratic nonlinear terms arise from the solution-dependent matrices $\mathbf{K}_{12(NL)}$, $\mathbf{K}_{21(NL)}$, $\mathbf{K}_{45(NL)}$ and $\mathbf{K}_{54(NL)}$. Cubic nonlinearities are represented by the matrices $\mathbf{K}_{22(NL)}$ and $\mathbf{K}_{55(NL)}$, which exhibit quadratic dependency on the solution. Additionally, the matrices $\mathbf{K}_{22(k_{NL})}^{disc.}$ and $\mathbf{K}_{24(k_{NL})}^{disc.}$ depend cubically on the solution, highlighting the nonlinear characteristics of the system. Furthermore, the influence of the elastic layer's stiffness, including the discontinuity, is described by the matrices $\mathbf{K}_{22(k_L)}^{disc.}$, $\mathbf{K}_{22(k_{NL})}^{disc.}$ and $\mathbf{K}_{24(k_{NL})}^{disc.}$. Damping is modeled using Rayleigh proportional damping with coefficients $\tilde{\alpha}$ and $\tilde{\beta}$. The equations of motion are reformulated into a more compact notation for efficiency in further analysis

$$\mathrm{M}\ddot{\mathrm{q}}(t) + \tilde{\alpha}(\mathrm{K}_{\ell})\dot{\mathrm{q}}(t) + \tilde{\beta}(\mathrm{M})\dot{\mathrm{q}}(t) + \left(\mathrm{K}_{\ell} + \mathrm{K}_{\mathrm{n}\ell}\big(\mathrm{q}(t)\big)\right)\mathrm{q}(t) = \mathrm{F}(t) \tag{8}$$

Each displacement component corresponds to a distinct set of shape functions. The transverse displacement is represented using a combination of Legendre polynomials, expressed in Rodrigues' form, and four Hermite cubic functions. Among these, only one Hermite cubic function at the ends of each element exhibits a non-zero value for either displacement or rotation, while the higher-order Legendre polynomials have zero amplitudes and slopes at $\xi = \pm 1$. For longitudinal displacements and rotations, a specific set of polynomials, referred to as the g-set, is used alongside linear functions. These g-functions have a zero value at the boundaries, but their slopes are non-zero.

In the numerical simulation involving time-domain analysis, the generalized external force vector, $\mathbf{F}(t) = \{0,\ 0,\ 0,\ 0,\ \mathbf{F}_{w2}, 0\}$, is defined as a time-dependent function representing the harmonic excitation applied transversely to the upper beam. This explicit time dependency highlights the non-autonomous nature of the systems under study, which are subjected to harmonic forces. The scenarios analyzed include clamped-clamped double beam system with and without asymmetric discontinuity in the Winkler layer, and their dynamic behavior is thoroughly examined.

2.1 The effect of an asymmetric discontinuity in the Winkler layer on the natural frequencies

The p-version FEM approach is utilized to evaluate the comparison of results between symmetric and asymmetric beam-beam systems with clamped-clamped boundary conditions. This analysis incorporates additional variations in geometric and material characteristics of the system, which are defined as follows.

$$L_i = 10\ \mathrm{m},\ A_i = 5 \times 10^{-2}\ \mathrm{m}^2,\ \rho_i = 2 \times 10^3\ \mathrm{kgm}^{-3}, k = 2 \times 10^5\ \frac{\mathrm{N}}{\mathrm{m}^2}, E_i = 1 \times 10^{10}\ \mathrm{Nm}^{-2},$$

$$I_i = 4 \times 10^{-4}\mathrm{m}^4,\ \lambda_i = \frac{5+5\nu}{6+5\nu},\ \nu_i = 0.34, i = 1, 2. \tag{9}$$

This section presents a set of frequencies illustrating the variation of the second coupled frequency depending on the existence of an asymmetric Winkler layer. The tabular representation provides insights into the reduction of the coupled frequency when the asymmetric layer is included in the model. Within the framework of different models shown in Figures 1a and 1b, corresponding respectively to cases a and b in the table, it is evident that the asymmetry of the Winkler layer plays a significant role in altering the natural frequencies. However, this is insufficient for a more detailed analysis of the dynamic behavior of the entire system, as well as its maximum deformation in the steady-state regime of forced oscillations, especially when all nonlinear effects are considered. The tabular data is provided to highlight the changes in the coupled frequency and its quantitative characteristics.

Table 1
Natural frequencies (rad/s) of a clamped-clamped double-beam system with asymmetric layer
(a) and classical double-beam system
(b) number of used shape functions: $p(g, f, \theta) = 6$.

Case	Freq.	Mode number	
		n=1	n=2
a	ω_{11}	44.4678	121.627
	ω_{12}	58.4913	136.519
b	ω_{11}	44.4678	121.627
	ω_{12}	50.1296	127.478

3. Geometrically nonlinear vibrations in the time domain

This section explores the influence of forced nonlinear vibrations using numerical simulations conducted in the time domain. The equations of motion were solved utilizing the Newmark method. The excitation force was modeled as a harmonic function of time, expressed as $f(t) = F\cos(\omega_e\, t)$, where ω_e denotes the excitation frequency and F represents the amplitude. A summary of results from various scenarios, as outlined in Table 1, is provided. The analysis considers an excitation amplitude of $(F = 50 \cdot 10^3\text{N})$ and a frequency $(\omega = 0.9\omega_{\ell 1})$, applied at the mid-span of the system. Initially, experimental results from Wolfe [31] were compared with the numerical results from Stojanović *et al.* [27] to validate the accuracy of the computational approach. This comparison was performed using identical geometric and material properties for the beam. Subsequently, the mechanical system incorporating an elastic layer, consistent with (Hao [6], Stojanović *et al.* [32]), was further analyzed, including the influence of an asymmetric Winkler layer. Time histories and phase plots for cases a and b are shown in Figures 2 and 3, respectively. Figure 4 illustrates the deformation shapes of the beams under maximum amplitudes at various points during the steady-state regime of forced nonlinear vibrations.

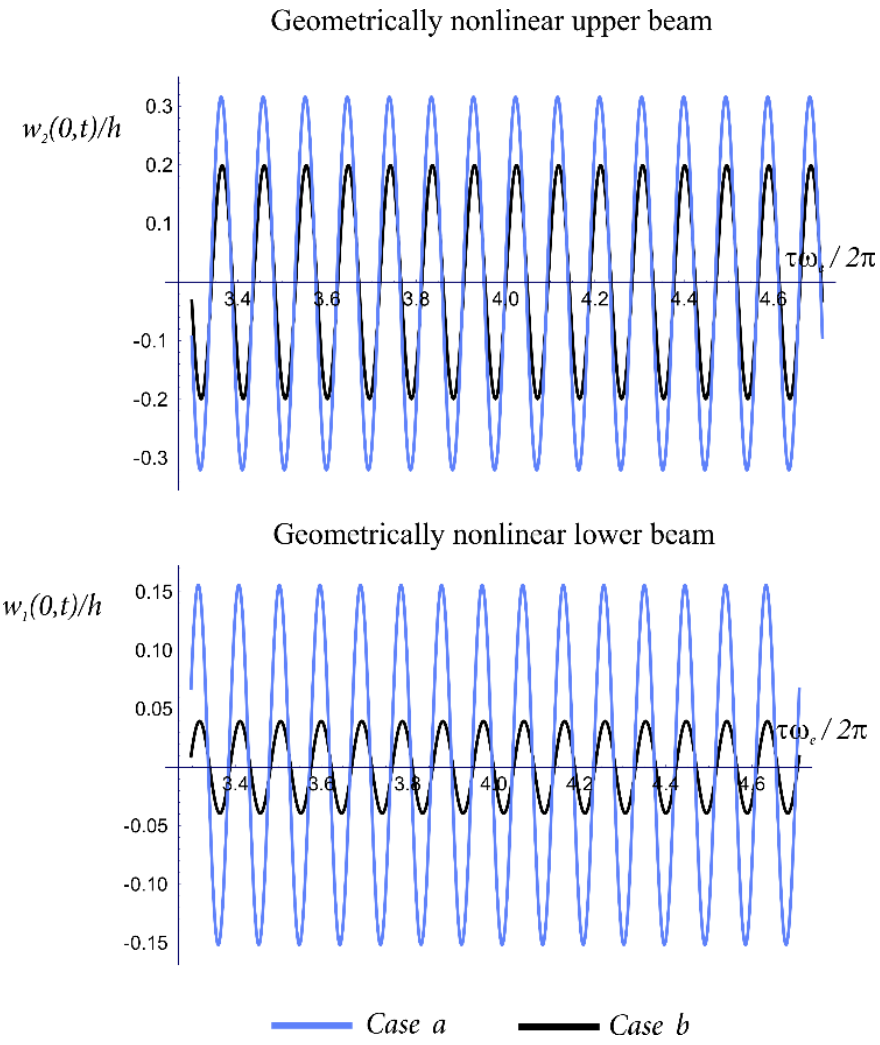

Fig. 2. Comparison of the time histories at the midpoints of the double-beam system with an asymmetrical Winkler layer (Case a) and the classical double-beam system (Case b).

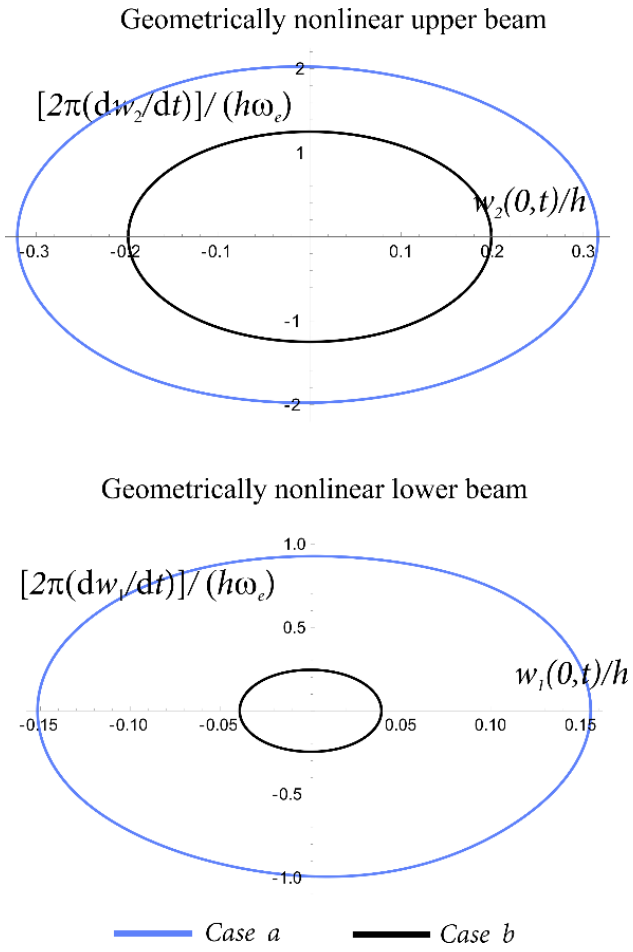

Fig. 3. Comparison of the phase plots at the midpoints of the double-beam system with an asymmetrical Winkler layer (Case a) and the classical double-beam system (Case b).

Figure 2 demonstrates that the presence of an asymmetric Winkler layer significantly amplifies the vibration amplitudes of both beams. Specifically, the asymmetric layer leads to a more pronounced increase in the upper beam's amplitudes. However, the difference becomes even more notable when comparing the maximum amplitudes of the lower beam with and without the asymmetric layer (blue line, case a, versus black line, case b). This observation suggests that, despite the applied force being on the upper beam, the most significant disparity in steady-state amplitudes occurs on the lower beam. This finding is particularly relevant and can be applied to the design of various asymmetric structural configurations.

Figure 3 presents phase plots that include the velocities of the beam midpoints. The key observation here is the increase in velocity caused by the presence of the asymmetric Winkler layer. The trends in velocity changes closely align with those in amplitude changes. The phase plots reveal a much greater velocity difference at the midpoint of the lower beam when the asymmetric Winkler layer is present compared to the case without it. Conversely, the difference in velocity changes for the upper beam is less pronounced.

Figure 4 provides a comparative visualization of the deformation shapes for cases a and b, highlighting the maximum amplitudes at all points along the beams. Several conclusions can be drawn from these observations, which could guide further analyses of similar asymmetric coupled

structures. The first conclusion pertains to the asymmetry of maximum deformation in the upper beam, which shifts toward the side lacking the Winkler layer. At this position, the deformation shows the largest deviation compared to the scenario where the Winkler layer is continuous (case bb). For the lower beam, the behavior is even more intriguing. The presence of an asymmetric Winkler layer induces a local deformation maximum on the opposite side of the beam, relative to the absence of the layer. Additionally, the lower beam exhibits significantly greater differences in maximum deformations across all points when comparing cases with and without the asymmetric Winkler layer. These findings underscore the pronounced impact of the asymmetric Winkler layer on deformation asymmetry in the lower beam during the steady-state regime of forced vibrations. Furthermore, the results emphasize that such asymmetries could serve as critical factors in the design and stability of coupled mechanical systems.

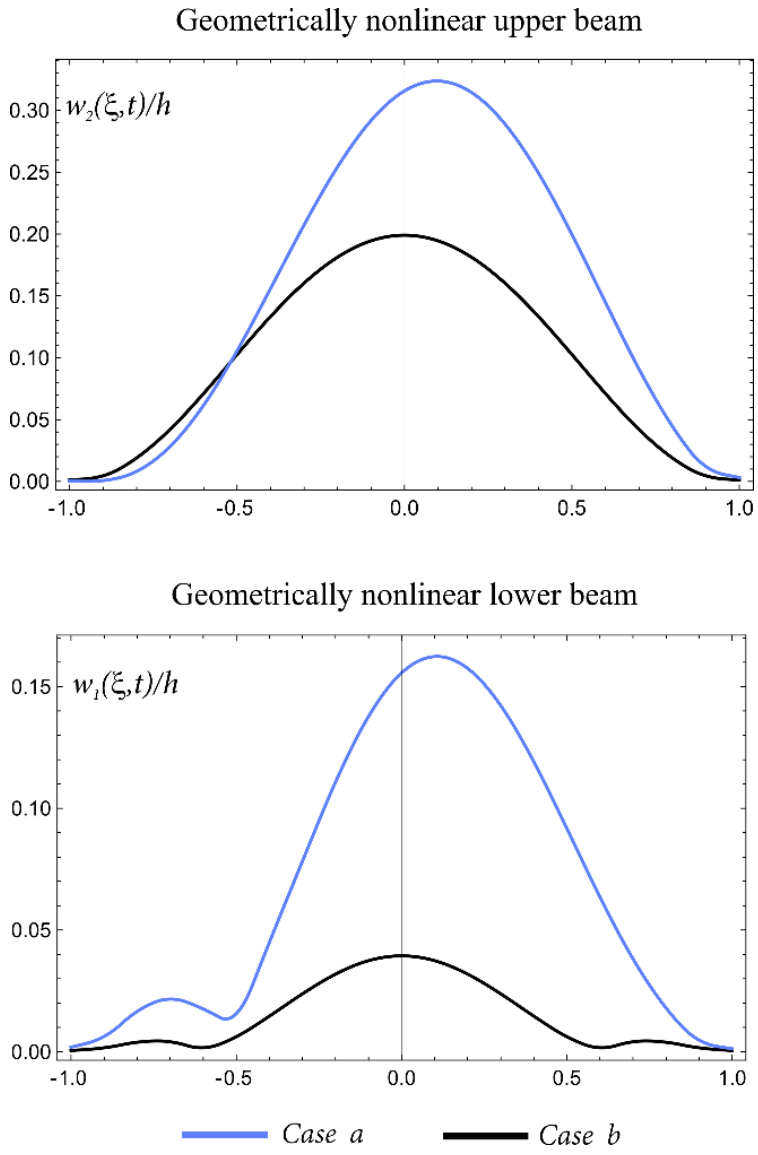

Fig. 4. Comparison of the maximum deflections during forced nonlinear vibrations between the double-beam system with an asymmetrical Winkler layer (Case a) and the classical double-beam system (Case b)

4. Conclusions

This study highlights the significant impact of an antisymmetric discontinuity in a Winkler nonlinear elastic layer on the dynamic behavior of a double Timoshenko beam system. Incorporating geometric nonlinearity and utilizing a modified p-version finite element method, the research provides a detailed time-domain analysis of forced vibrations in systems with discontinuities. The findings reveal that the asymmetric Winkler layer amplifies vibration amplitudes in both beams, with the upper beam experiencing more pronounced increases, while the lower beam exhibits the greatest disparity in steady-state amplitudes between cases with and without the layer. Phase plot analyses indicate that the asymmetric layer significantly increases velocity variations, particularly in the lower beam, aligning with trends in amplitude changes and underscoring its influence on dynamic stability. Deformation shapes further emphasize the asymmetry caused by the Winkler layer, with the upper beam's maximum deformation shifting toward the side without the layer and the lower beam showing localized deformation maxima. These results underscore the critical role of the discontinuity in altering oscillatory behavior, deformation, and velocity profiles. Practical implications include the potential use of such discontinuities to optimize dynamic responses in coupled structures, offering insights for stabilizing and controlling mechanical systems in technical applications. This work provides a foundation for advancing the design of asymmetric elastic layers in deformable bodies and coupled systems.

Author Contributions

Conceptualization, Methodology, Software, Writing, D.M.; Supervision, Writing - Review & Editing, Validation, Project administration, J.D.; Methodology, Software, Writing, D.L. Conceptualization, Methodology, Software, Writing, V.S. All authors have read and agreed to the published version of the manuscript.

Funding

This research received no external funding.

Data Availability Statement

Not applicable.

Conflicts of Interest

The authors declare that they have no known competing financial interests or personal relationships that could have appeared to influence the work reported in this paper.

Acknowledgement

We acknowledge the financial support from Natural Sciences and Engineering Research Council of Canada through discovery grants and from the Government of Canada's New Frontiers in Research Fund (NFRF) [NFRFR-2021-00262] and research was also financially supported by the Ministry of Science, Technological Development and Innovation of the Republic of Serbia (Contract No. 451-03-47/2023-01/ 200109).

References

[1] Rezaei, M., Talebitooti, R., & Liao, W.-H. (2022). Concurrent energy harvesting and vibration suppression utilizing PZT-based dynamic vibration absorber. *Archive of Applied Mechanics*, 92, pp. 363-382. https://doi.org/10.1007/s00419-021-02063-4.

[2] Ari, M., & Faal, M. (2019). Passive vibration suppression of plate using multiple optimal dynamic vibration absorbers. *Archive of Applied Mechanics*, 90, pp. 235–274. https://doi.org/10.1007/s00419-019-01607-z.

[3] Zhang, S. Q., Gao, Y. S., Pu, H. Y., Wang, M., Ding, J. H., & Sun, Y. (2021). Numerical modeling for viscoelastic sandwich smart structures bonded with piezoelectric materials. *Composite Structures*, 278, 114703. https://doi.org/10.1016/j.compstruct.2021.114703.

[4] Kennedy, D., Cheng, R. K. H., Wei, S., & Alcazar Arevalo, F. J. (2016). Equivalent layered models for functionally graded plates. *Computers & Structures*, 174, pp. 113-121. https://doi.org/10.1016/j.compstruc.2015.09.009.

[5] Stojanović, V., Petković, M. D., & Deng, J. (2019). Stability of parametric vibrations of an isolated symmetric cross-ply laminated plate. *Composites Part B: Engineering*, 167, pp. 631-642. https://doi.org/10.1016/j.compositesb.2019.02.041.

[6] Hao, N., Zhu, L., Wu, Z., & Ke, L. (2023) Softening-spring nonlinearity in large amplitude vibration of unsymmetric double-layer lattice truss core sandwich beams. *Thin-Walled Structures*, 182 (Part A), 110164. https://doi.org/10.1016/j.tws.2022.110164.

[7] Zhang, Q. Y., Lu, Y., Wang, L. S., & Liu, X. (2010) Vibration and buckling of a double-beam system under compressive axial loading. *Journal of Sound and Vibration*, 318, pp. 341-352. https://doi.org/10.1016/j.jsv.2008.03.055.

[8] Li, X. Y., & Gong, J. (2022). Free and forced vibration analysis of general multiple beam systems. *International Journal of Mechanical Sciences*, 235, 107716. https://doi.org/10.1016/j.ijmecsci.2022.107716.

[9] Ghomshei, M. M. (2020). A numerical study on the thermal buckling of variable thickness Mindlin circular FGM plate on a two-parameter foundation. *Mechanics Research Communications*, 108, pp. 103577. https://doi.org/10.1016/j.mechrescom.2020.103577.

[10] Bochicchio, I., Giorgi, C., & Vuk, E. (2016). Buckling and nonlinear dynamics of elastically coupled double-beam systems. *International Journal of Non-Linear Mechanics*, 85, pp. 161–173. https://doi.org/10.1016/j.ijnonlinmec.2016.06.009.

[11] Hajarolasvadi, S., & Elbanna, A. E. (2019). Dynamics of metamaterial beams consisting of periodically-coupled parallel flexural elements: a theoretical study. *Journal of Physics D: Applied Physics*, 52, pp. 315101. http://dx.doi.org/10.1088/1361-6463/ab1f9e.

[12] Adam, C., & Furtmüller, T. (2020). Flexural vibrations of geometrically nonlinear composite beams with interlayer slip. *Acta Mechanica*, 231, pp. 251–271. https://doi.org/10.1007/s00707-019-02528-2.

[13] Palmeri, A., & Adhikari, S. (2011) A Galerkin-type state-space approach for transverse vibrations of slender double-beam systems with viscoelastic inner layer. *Journal of Sound and Vibration*, 330(26), pp. 6372-6386. http://dx.doi.org/10.1016/j.jsv.2011.07.037.

[14] Xin, Y., Cui, C., Liu, H., Wang, B., Xu, C., Xu, Li., & Fu, G. (2024). Dynamic analysis for horizontal vibration of piles in layered Pasternak soils considering secondary ground waves. *Soil Dynamics and Earthquake Engineering*, 187, 109026. https://doi.org/10.1016/j.soildyn.2024.109026.

[15] Zhou, Y. R., Yan, X.B., Wang, M.X., Liu, Y.C., & Wen, P.H. (2024). Dynamic fundamental solution of dipole for Kirchhoff plate on Winkler-Pasternak foundation. *Computers & Structures*, 304, 2024, 107498. https://doi.org/10.1016/j.soildyn.2024.109026.

[16] Mazur-Śniady, K., Misiurek, K., Szyłko-Bigus, O., & Śniady, P. (2013). Fuzzy Stochastic Vibrations of Double-Beam Complex System as Model Sandwich Beam with Uncertain Parameters. *ISRN Applied Mathematics*, 2013, pp. 1–12. http://dx.doi.org/10.1155/2013/340145.

[17] Mohammadzadeh, S., Esmaeili, M., & Mehrali, M. (2013). Dynamic response of double beam rested on stochastic foundation under harmonic moving load. *International Journal for Numerical and Analytical Methods in Geomechanics*, 38(6), pp. 572–592. https://doi.org/10.1002/nag.2227.

[18] Di Lorenzo, S., Adam, C., Burlon, A., Failla, G., & Pirrotta, A. (2018). Flexural vibrations of discontinuous layered elastically bonded beams. *Composites Part B: Engineering*, 135, pp. 175–188. https://doi.org/10.1016/j.compositesb.2017.09.059.

[19] Juarez, G., & Ayala, A. G. (2012). Finite element variational formulation for beams with discontinuities. *Finite Elements in Analysis and Design*, 54, pp. 37–47. https://doi.org/10.1016/j.finel.2012.01.004.

[20] Srikarun, B., Songsuwan, W., & Wattanasakulpong, N. (2021). Linear and nonlinear static bending of sandwich beams with functionally graded porous core under different distributed loads. *Composite Structures*, 276, 114538. https://doi.org/10.1016/j.compstruct.2021.114538.

[21] Songsuwan, W., Wattanasakulpong, N., & Kumar, S. (2023). Nonlinear transient response of sandwich beams with functionally graded porous core under moving load. *Engineering Analysis with Boundary Elements*, 155, pp. 11–24.

[22] Bitar, I., Kotronis, P., Benkemoun, N., & Grange, S. (2018). A generalized Timoshenko beam with embedded rotation discontinuity. *Finite Elements in Analysis and Design*, 150, pp. 34–50. https://doi.org/10.1016/j.finel.2018.07.002.

[23] Szabó, B., & Babuška, I. (1991). Finite Element Analysis. *John Wiley & Sons*, New York. https://doi.org/10.2307/2153181.
[24] Petyt, M. (1990). Introduction to Finite Element Vibration Analysis. *Cambridge University Press*. https://doi.org/10.1017/CBO9780511761195.
[25] Han, W., & Petyt, M. (1996). Linear vibration analysis of laminated rectangular plates using the hierarchical finite element method, Part 1: free vibration analysis. *Computers & Structures*, 61, pp. 705–712. https://doi.org/10.1016/0045-7949(96)00213-1.
[26] Bardell, N. S. (1989). The application of symbolic computing to the hierarchical finite element method. *International Journal for Numerical Methods in Engineering*, 28, pp. 1181–1204. https://doi.org/10.1002/nme.1620280513.
[27] Stojanović, V., Ribeiro, P., & Stoykov, S. (2013). Non-linear vibration of Timoshenko damaged beams by a new p-version finite element method. *Computers & Structures*, 120, pp. 107–119. https://doi.org/10.1016/j.compstruc.2013.02.012.
[28] De Rosa, M. A. (1995). Free vibrations of Timoshenko beams on two-parameter elastic foundation. *Computers & Structures*, 57, pp. 151–156. https://doi.org/10.1016/0045-7949(94)00594-S.
[29] Ariaei, A., Ziaei-Rad, S., & Ghayour, M. (2010). Transverse vibration of a multiple-Timoshenko beam system with intermediate elastic connections due to a moving load. *Archive of Applied Mechanics*, 81(3), pp. 263–281. https://doi.org/10.1007/s00419-010-0410-2.
[30] ANSYS Workbench User's Guide, 2009. file:///C:/Users/Dunja/Downloads/WorkbenchUsersGuide.pdf.
[31] Wolfe, H. (1995). An experimental investigation of nonlinear behaviour of beams and plates excited to high levels of dynamic response. *PhD thesis*, *University of Southampton*. Southampton.
[32] Stojanović, V., Petković, M. D., & Milić, D. (2020). Nonlinear vibrations of a coupled beam-arch bridge system. *Journal of Sound and Vibration*, vol. 464, 115000. https://doi.org/10.1016/j.jsv.2019.115000.